

# **FRACTURE MECHANICS for CERAMICS, ROCKS, and CONCRETE**

**Freiman/Fuller, *editors***

**ASTM STP 745**

**AMERICAN SOCIETY FOR  
TESTING AND MATERIALS**

# FRACTURE MECHANICS FOR CERAMICS, ROCKS, AND CONCRETE

A symposium  
sponsored by ASTM  
Committee D-18 on  
Soil and Rock for  
Engineering Purposes  
and Committee E-24  
on Fracture Testing  
AMERICAN SOCIETY FOR  
TESTING AND MATERIALS  
Chicago, Ill., 23-24 June 1980

ASTM SPECIAL TECHNICAL PUBLICATION 745  
S. W. Freiman and  
E. R. Fuller, Jr.,  
National Bureau of Standards,  
editors

ASTM Publication Code Number (PCN)  
04-745000-30



AMERICAN SOCIETY FOR TESTING AND MATERIALS  
1916 Race Street, Philadelphia, Pa. 19103

Copyright © by AMERICAN SOCIETY FOR TESTING AND MATERIALS 1981  
Library of Congress Catalog Card Number: 81-65837

NOTE

The Society is not responsible, as a body,  
for the statements and opinions  
advanced in this publication.

Printed in Baltimore, Md.  
October 1981

## Foreword

The symposium on Fracture Mechanics for Ceramics, Rocks, and Concrete was presented at Chicago, Illinois, 23-24 June 1980. The symposium was sponsored by the American Society for Testing and Materials through its Committee D-18 on Soil and Rock for Engineering Purposes and Committee E-24 on Fracture Testing. S. W. Freiman and E. R. Fuller, Jr., National Bureau of Standards, are editors of this publication. Mr. Freiman also presided as chairman of the symposium.

## Related ASTM Publications

Crack Arrest Methodology and Applications, STP 711 (1980), \$44.75,  
04-711000-30

Fracture Mechanics, 12th Conference, STP 700 (1980), \$53.25, 04-700000-30

Part-Through Crack Fatigue Life Prediction, STP 687 (1979), \$26.25,  
04-687000-30

Fracture Mechanics Applied to Brittle Material, 11th Conference, STP 678  
(1979), \$25.00, 04-578000-30

Fracture Mechanics, 11th Conference, STP 677 (1979), \$60.00, 04-677000-30

Behavior of Deep Foundations, STP 670 (1979), \$49.50, 04-670000-38

Dynamic Geotechnical Testing, STP 654 (1978), \$34.50, 04-654000-38

Dispersive Clays, Related Piping, and Erosion in Geotechnical Projects, STP  
623 (1977), \$40.75, 04-623000-38

## A Note of Appreciation to Reviewers

This publication is made possible by the authors and, also, the unheralded efforts of the reviewers. This body of technical experts whose dedication, sacrifice of time and effort, and collective wisdom in reviewing the papers must be acknowledged. The quality level of ASTM publications is a direct function of their respected opinions. On behalf of ASTM we acknowledge with appreciation their contribution.

*ASTM Committee on Publications*

## Editorial Staff

Jane B. Wheeler, *Managing Editor*  
Helen M. Hoersch, *Senior Associate Editor*  
Helen P. Mahy, *Senior Assistant Editor*  
Allan S. Kleinberg, *Assistant Editor*

# Contents

<b>Introduction</b>	<b>1</b>
<b>Experimental Observation of Crack Velocity and Crack Front Shape Effects in Double-Torsion Fracture Mechanics Tests—T. A. MICHALSKE, M. SINGH, AND V. D. FRECHETTE</b>	<b>3</b>
<b>Determination of High-Temperature <math>K_{I-V}</math> Data for Si-Al-O-N Ceramics—M. H. LEWIS AND B. S. B. KARUNARATNE</b>	<b>13</b>
<b>Fracture Toughness of Glass Using the Indentation Fracture Technique—S. S. SMITH, P. MAGNUSEN, AND B. J. PLETKA</b>	<b>33</b>
<b>Application of Single Edge Notched Beam and Indentation Techniques to Determine Fracture Toughness of Alpha Silicon Carbide—M. SRINIVASAN AND S. G. SESHADRI</b>	<b>46</b>
<b>Effect of Stable Crack Growth on Fracture Toughness Determination for Hot-Pressed Silicon Nitride at Elevated Temperatures—D. MUNZ, G. HIMSLT, AND J. ESCHWEILER</b>	<b>69</b>
<b>Precracking of Fracture Toughness Specimens by Wedge Indentation—E. A. ALMOND AND B. ROEBUCK</b>	<b>85</b>
<b>Test-Microstructural Dependence of Fracture Energy Measurements in Ceramics—R. W. RICE</b>	<b>96</b>
<b>Specimen Size Effects in Fracture Toughness Testing of Heterogeneous Ceramics by the Notch Beam Method—K. R. MCKINNEY AND R. W. RICE</b>	<b>118</b>
<b>The Character of Cracks in Fracture Toughness Measurements of Ceramics—C. Cm. WU, R. W. RICE, AND P. F. BECHER</b>	<b>127</b>
<b>Compliance Measured Fracture Toughness of Mortar and Fiber Reinforced Mortar—K. VISALVANICH AND A. E. NAAMAN</b>	<b>141</b>
<b>Relationship Between Differential Stress Intensity Factor and Crack Growth Rate in Cyclic Tension in Westerly Granite—KUNSOO KIM AND ABDUL MUBEEN</b>	<b>157</b>



<b>Static and Dynamic Fracture Behavior of Oil Shale—L. S. COSTIN</b>	169
<b>Application of the Hopkinson Split Bar Test to the Mechanical and Fracture Properties of Rocks—JAROSLAV BUCHAR AND ZDENĚK BÍLEK</b>	185
<b>Precursors of Laboratory Rock Failure—G. A. ROWELL, B. T. BRADY, L. P. YODER, AND D. R. HANSON</b>	196
<b>Fracture Mechanics of Crack Bands in Concrete—LUIGI CEDOLIN AND Z. P. BAŽANT</b>	221
<b>Extension of the Compliance and Stress Intensity Formulas for the Single Edge Crack Round Bar in Bending—FINN OUCHTERLONY</b>	237
<b>Consequences of Varying Surface Heat Transfer Coefficients, Material Properties, and Cyclical Ambient Temperatures upon Stress Intensity Factors for Edge Cracks—A. F. EMERY, A. S. KOBAYASHI, AND T. R. BIELER</b>	257
<b>Summary</b>	273
<b>Index</b>	277

# Introduction

---

This volume "Fracture Mechanics Techniques for Ceramics, Rocks, and Concrete" represents the proceedings of a symposium organized by ASTM Subcommittee E24.07 and ASTM Committee D18. It is a continuation of the effort to characterize and understand the important parameters pertinent to the testing of brittle materials, which was begun in *STP 678, Fracture Mechanics Applied to Brittle Materials*. This compilation of papers emphasizes the use of current fracture mechanics models to understand the failure of important engineering materials such as concrete, SiC, Si<sub>3</sub>N<sub>4</sub>, and Si-Al-O-N's. The continued development of test techniques specifically designed for brittle materials is discussed throughout a large number of papers in this collection.

As will be seen from a number of these papers, fracture mechanics is also finding an important place in the prediction of failures in large-scale geologic formations based on results of laboratory scale tests. This volume should provide the reader with a good feeling of the state of the science of brittle failure in many of the above areas. It is one step along the road toward a complete understanding of this complex problem.

Finally, thanks must be given to A. I. Johnson and Howard Pincus of Committee D-18, who helped in the organization of the symposium.

*S. W. Freiman*

*E. R. Fuller, Jr.*

Fracture and Deformation Division, National  
Bureau of Standards, Washington, D.C.  
20234, editors.



## Experimental Observation of Crack Velocity and Crack Front Shape Effects in Double-Torsion Fracture Mechanics Tests

---

**REFERENCE:** Michalske, T. A., Singh, M., and Frechette, V. D., "Experimental Observation of Crack Velocity and Crack Front Shape Effects in Double-Torsion Fracture Mechanics Tests," *Fracture Mechanics Methods for Ceramics, Rocks, and Concrete, ASTM STP 745*, S. W. Freiman and E. R. Fuller, Eds., American Society for Testing and Materials, 1981, pp. 3-12.

**ABSTRACT:** The double-torsion test configuration has been used to obtain crack growth information for a variety of materials. Recently critical reviews have suggested that certain assumptions used in the interpretation of double-torsion data are of questionable validity.

This paper presents experimental data for crack growth in glass specimens loaded in the double-torsion test configuration. The constant displacement rate technique was used to propagate cracks and velocity was measured continuously by superimposing a tuned-frequency sonic signal during cracking. The crack velocity profile as a function of position along the crack front was determined. The crack velocity at the tensile surface was measured as a function of crack length at constant load and the crack front shape was observed for various crack lengths.

**KEY WORDS:** double torsion testing, fractography, glass fracture mechanics, crack propagation, composite materials

The double torsion (DT) method for obtaining crack growth data ( $\log V$  vs.  $K_I$ ) was first suggested by Outwater and Gerry [1]<sup>4</sup> and later developed by Kies and Clark [2] and Williams and Evans [3]. Experimental observations have shown that the DT technique produces an asymmetric crack front shape. Shetty, Virkar, and Harward [4] suggested that the crack front shape in double torsion specimens may affect crack growth data and have proposed a

<sup>1</sup> Ceramic engineer, National Bureau of Standards, Washington, D.C. 20234.

<sup>2</sup> Mechanical engineer, Turbodyne Corp., Wellsville, N.Y. 14895.

<sup>3</sup> Professor, N.Y.S. College of Ceramics, Alfred University, Alfred, N.Y. 14802.

<sup>4</sup> The italic numbers in brackets refer to the list of references appended to this paper.

correction factor to be applied to results from double torsion specimens. Pletka, Fuller, and Koepke [5] and Fuller [6] reviewed DT procedures, experimental data, and analytical justification for DT testing. In their papers, the need to verify some basic assumptions associated with DT testing was pointed out.

The purpose of this work was to measure experimentally the crack front profile and crack velocity effects which occur during crack growth in DT specimens. Results from these measurements will be discussed in terms of stress intensities for DT cracks, assumptions used in the analysis of DT specimens, and the validity of DT crack growth data.

### Procedure

Specimens for this study were edge cracked soda-lime-silica glass plates measuring 3.0 by 30.0 by 90.0 mm (Fig. 1). Edge cracks  $\sim 20.0$  mm long were produced parallel with the long dimension of the specimen by a hot wire technique [7].

A loading fixture similar to that described by Pletka et al [5] was used to stress the specimens in the double torsion configuration. Tests were conducted using the constant displacement rate technique [8]. The DT apparatus (Fig. 2) was loaded in an Instron testing machine at a crosshead speed of 0.005 cm/min.

Crack velocity and crack front shape were measured with two techniques modified from Kerkhof's [9] method of ultrasonic fractography. This method relies on perturbation of the crack direction by elastic impulses to form Wallner lines on the fracture generated surface. Post-mortem measurement of the spacing between Wallner lines is used to calculate crack velocity. Crack front shape information is given directly by the shape of the Wallner lines since the crack velocity is much less than the elastic wave velocity in these experiments. In one technique, the Wallner lines were produced by the interaction of the crack tip stresses with trains of tuned frequency

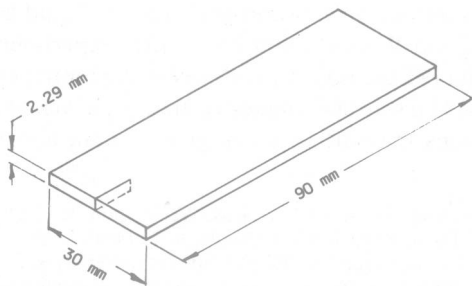


FIG. 1—Specimen geometry.

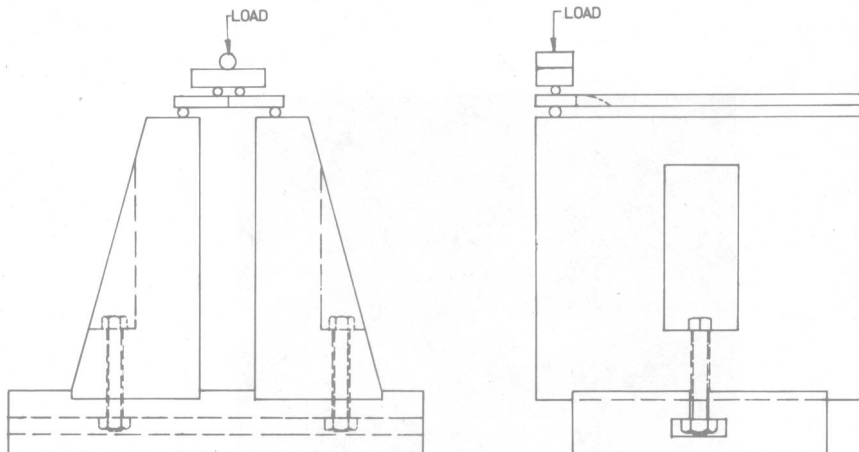


FIG. 2—Constant displacement rate loading rig.

shear waves [10]. The second technique utilized low-frequency impulses which resulted from mechanical tapping to develop the Wallner lines. The method of ultrasonic fractography offers advantages over other methods used to measure crack velocity and crack front shape effects. Wallner lines allow the determination of crack velocity at all parts of the crack whereas optical measurements only yield the velocity at one portion of the crack front. The crack fronts illustrated by Wallner lines are representative of moving cracks whereas arrest lines (those lines caused by unloading then reloading the specimen) show the crack front shape which developed as the specimen was unloaded.

All experiments were conducted in room air at 30 percent relative humidity and 21°C and crack velocity was maintained at a sufficient level to ensure Region III crack growth behavior.

## Results

Double torsion crack front shapes as represented by Wallner lines on the fracture surface are displayed in Fig. 3. Crack front shape information taken from such photographs was digitized, and the data were fit by an equation of the form  $Y = a_0 + a_1 X + a_2 X^2$ . Figure 4 shows the coordinate system used in analyzing the data. Crack fronts were measured over approximately 75 percent of the specimen thickness because Wallner lines near the compressive surface were not clear enough for accurate readings. (For the purpose of this study it is reasoned that crack extension occurring near the compressive surface has little effect on crack growth data.) Profiles of five different crack fronts over the load plateau were analyzed in this manner.

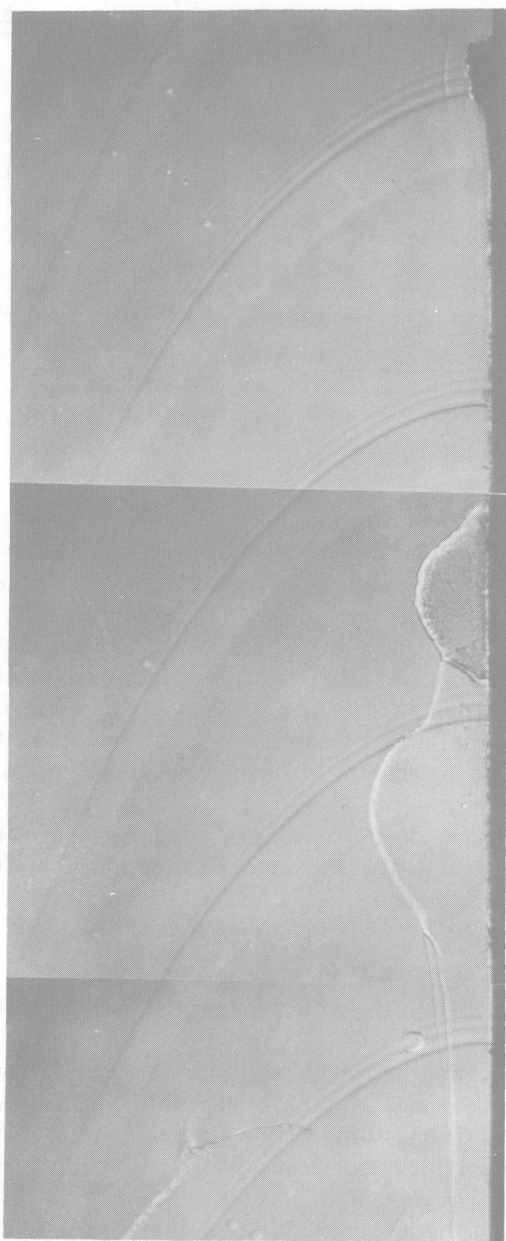


FIG. 3—Fracture surface showing double torsion crack fronts. Crack direction left to right. Differential interference contrast,  $\times 20$ .

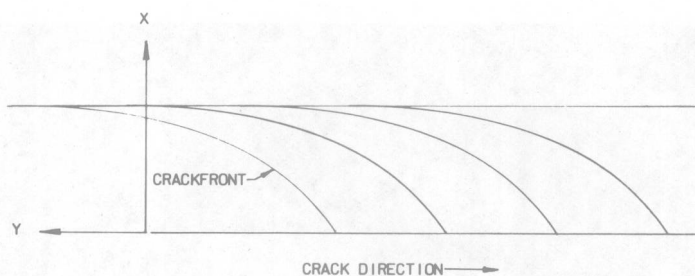


FIG. 4—Coordinate system for curve fitting.

Table 1 shows the polynomial coefficients and the coefficient of correlation for each successive crack front.  $a_0$  reflects the position of the crack's leading edge,  $a_1$  is related to position in the  $X$  direction, and  $a_2$  defines the shape of each curve. Since each crack front is further along the specimen, the  $a_0$  coefficient is larger for each successive curve. Values for  $a_1$  are nearly zero and probably represent alignment errors in digitizing the data. The  $a_2$  coefficients are nearly equal showing that each successive crack front maintained a constant shape.

Finally, the nearly perfect coefficient of correlation shows that the DT crack front can be described by a parabolic equation. Figure 5 shows a DT specimen where an inclusion was intersected by the crack plane. The lancet of hackle trailing the inclusion points in the direction of local fracture and shows that on a local scale the fracture moves normal to the crack front. Since the local direction is normal to the crack front, curves normal to successive crack fronts were generated to show the fracture path in a DT specimen (Fig. 6). The local velocity along the DT crack front was calculated from measurements of the normal distance between consecutive crack fronts. These local or absolute velocities were used to calculate the  $X$  and  $Y$  components of crack velocity.

Figure 7 shows the  $X$  component,  $Y$  component, and absolute velocity plotted as a function of the angle ( $\theta$ ) between the crack front normal and the specimen free surface. At the leading or tensile surface ( $\theta = 0$  deg) all of the crack velocity is in the  $Y$  component and at the trailing or compressive sur-

TABLE 1—Curve fit parameters for double torsion crack fronts.

$a_0$	$a_1$	$a_2$	Coefficient of Correlation
1.80	0.01	-0.41	0.999
3.68	-0.01	-0.41	0.999
5.55	-0.02	-0.41	0.999
7.37	0.00	-0.42	0.999
9.18	-0.05	-0.40	0.999



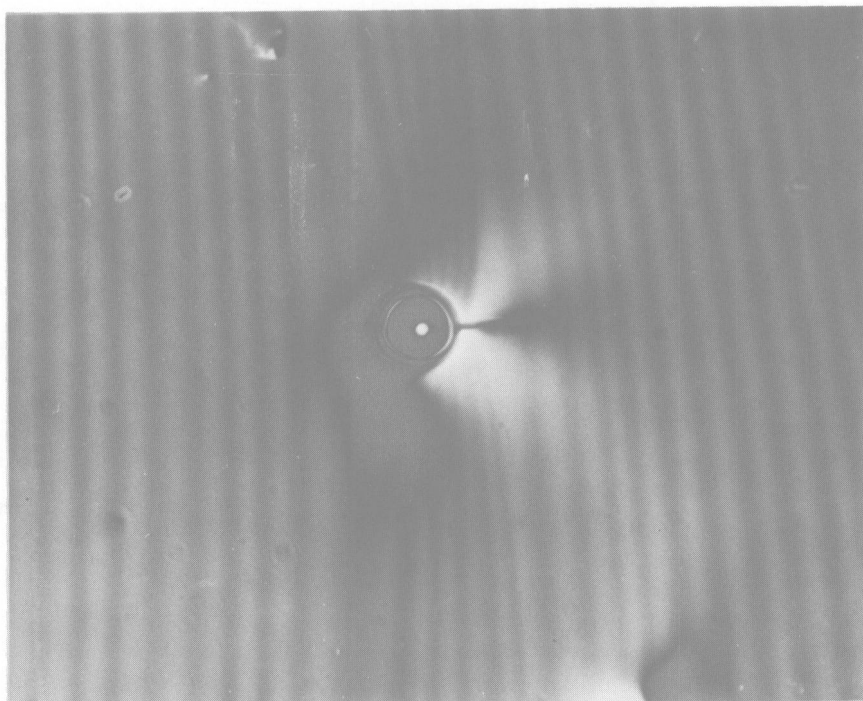


FIG. 5—Fracture surface showing intersection of inclusion by crack plane. Crack direction left to right. Differential interference contrast,  $\times 150$ .

face ( $\theta = 90$  deg) all components of velocity are zero. Over the extent of measurable crack front the absolute velocity varied by approximately a factor of four with the highest velocity at the tensile surface.

Crack velocity at the leading edge ( $\theta = 0$  deg) was also plotted as a function of crack length for the constant displacement rate experiments (Fig. 8). Figure 8 also shows the load diagram which corresponds to the crack velocity data.

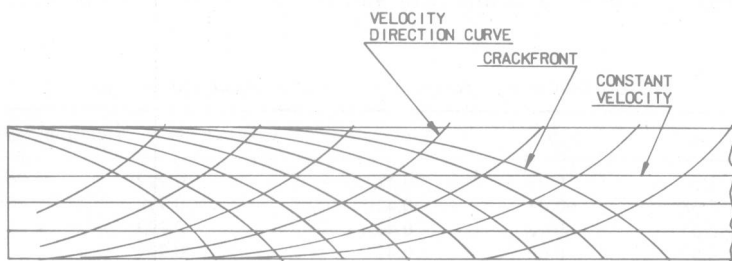


FIG. 6—Crack front, velocity direction, and constant velocity curves.